International Journal of Heat and Technology
Vol. 42, No. 5, October, 2024, pp. 1777-1786
Journal homepage: http://iieta.org/journals/ijht

Significance of Joule Heating and Fourier Heat Flux on the Dynamics of Ternary Hybrid Nanofluid Rotating in a Circular Porous Disk

Leela Santi Parige[1], Deevi Sateesh Kumar[1*], Gudala Balaji Prakash[2]

[1] Department of Engineering Mathematics, Koneru Lakshmaiah Education Foundation, Guntur 522302, India
[2] Department of Mathematics, Aditya University, Surampalem 533437, India

Corresponding Author Email: drskd@kluniversity.in

https://doi.org/10.18280/ijht.420532

Received: 4 July 2024
Revised: 25 September 2024
Accepted: 10 October 2024
Available online: 31 October 2024

Keywords:
hybrid nanofluid, Christov heat flux, thermal radiation, magnetic field

ABSTRACT

This study delves into the intriguing interplay between Fourier heat flux and Joule heating, exploring their effects on a ternary hybrid nanofluid caught in the rotational dance of a circular porous disk. It unpacks the roles of Joule heating, thermal radiation, heat generation, and viscous dissipation in shaping the dynamics of heat transfer. To untangle the complex behaviour of the system, we transformed the governing partial differential equations (PDEs) into ordinary differential equations (ODEs), paving the way for a clearer insight into the physical phenomena at play. We employed a numerical solution approach, showcasing the precision of the shooting method against established techniques in the field. Our results unveil a fascinating narrative: increased thermal radiation, heat generation, and viscous dissipation significantly enhance heat transfer efficiency, thickening the thermal boundary layer in the process. On the other hand, as the magnetic parameter increases, it restricts the flow of the electrically conducting fluid, which ultimately results in a decrease in the thickness of the momentum boundary layer. This interplay of forces reveals the delicate balance governing heat dynamics in this unique system.

1. INTRODUCTION

In order to investigate hybrid nanofluids, particularly ternary hybrids, it is necessary to combine nano-sized powders based on polymers or metallic materials with ordinary fluids. This forward-thinking approach has a wide range of applications, ranging from heat channels and solar energy systems to heat transfer and cooling solutions designed for a variety of different pieces of machinery. Ternary hybrid nanoparticles were selected for their outstanding thermophysical and rheological properties, serving as a solid foundation for further research. Utilizing two porous disks, Raza et al. [1] supervised an investigation into the impacts of nanolayers on the thermodynamics of tri-hybrid nanofluids. The purpose of this investigation was to expose the potential of nanolayers across a variety of applications.

While this was going on, Idowu and Falodun [2] investigated how the dynamics of nanoparticles are affected through the utilization of a vertical porous plate, which creates a presence of changing viscosity and heat conductivity. It was the objective of Salah et al. [3] to investigate the effects of PST and PHF heating limits on the swirl flow of an Al+Mg+TiO_2 mixture that was contained within a spinning cone. The nonlinear Boussinesq and Rosseland approximations were applied by Sajjan et al. [4] in order to provide clarity on the three-dimensional dynamics that are influenced by ternary nanoparticles. In conclusion, Khan et al. [5] conducted research on the dynamics of energy and mass transfer of hybrid nanofluids while they were contained within an extended cylinder that contained a magnetic dipole.

An investigation of the flow of mixed convective nanofluids along an inclined uneven surface was carried out by Haq et al. [6], taking into account both the heat source and the chemical reaction. Nanofluids' non-Newtonian dynamics were investigated by Gladys and Reddy [7] through the manipulation of viscosity and thermal conductivity. Gurrampati and Vijaya [8] investigated the Buongiomo model for magnetohydrodynamics (MHD) Casson nanofluids using Brownian and thermophoretic diffusion. In many applications in engineering, including mechanical engineering, chemical engineering, power engineering and aerospace engineering the fluid dynamics through a rotating porous disk is a scientific phenomenon. The improvement of heat transmission based on hybrid nanofluid dynamics that was caused by a porous rotary disk was the subject of research conducted by Alkuhayli [9]. Mishra et al. [10] have recently investigated the dynamics of electroosmotic MHD ternary hybrid Jeffery nanofluids flowing in a ciliated vertical channel. Alhowaity et al. [11] studied non-Fourier energy transmission in power law hybrid nanofluid flows over a moving sheet, while Alharbi et al. [12] investigated the stagnation point dynamics of hybrid nanofluids around a rotating sphere, considering thermophoretic diffusion and thermal radiation. Both studies were published in the journal Engineering and Science.

By investigating both nonlinear and linear mixed convection, Kanwal et al. [13] searched the complex dynamics of heat and mass transfer inside nanofluids, which provided new insights into the dynamics of these processes. Regarding

as a result of the forces of heat and mass transport in MHD nonlinear free convection of non-Newtonian fluids, Tharapatla et al. [14] concentrated their attention on the subject.

The recent study of ternary hybrid nanofluids aims to deepen our recognizing of heat and mass transfer phenomena, particularly regarding the innovative impacts of radiative effects. These nanofluids consist of micron-sized particles that form colloids, paving the way for applications in various technological fields such as climate control, structural airflow, biomedical engineering, and coolant systems in milling.

Alqawasmi et al. [15] hired a numerical approach to examine the dynamics of ternary hybrid nanofluids, incorporating nonlinear heat sources and sinks alongside a Fourier heat flux model. This innovative method allowed for a deeper understanding of heat transfer in these complex fluids. Similarly, In the study that was carried out by Famakinwa et al. [16], the researchers looked into the time-dependent and incompressible squeezing flow of a CuO-Al_2O_3 water-based hybrid nanofluid that was squeezed between two parallel plates. Increasing viscosity was the primary focus of the researchers as they investigated its effect on flow characteristics.

An further contribution to the understanding of thermal behavior in such mixtures was made by Choudhary et al. [17], who carried out a thermal analysis of the dynamics of ternary hybrid nanoparticles based on kerosene oil. Adnan et al. [18] conducted a different investigation in which they highlighted the significance of the Koo-Kleintics uer-Li model in terms of its ability to increase the thermal characteristics of nanofluids when subjected to the effect of a magnetic field. This study additionally highlighted the possibility for enhanced heat transfer efficiency.

Algehyne et al. [19] explored ternary hybrid nanofluid dynamics using a numerical approach that included varying diffusion rates and non-Fourier heat conduction concepts, thus expanding the theoretical framework of heat transfer. Additionally, Ramzan et al. [20] analyzed mixed convection dynamics of a MHD hybrid nanofluid past a stretching sheet, incorporating thermal slip and velocity constraints to understand their impact on heat transmission.

For the purpose of shedding light on the intricate behavior of these fluids, Bayones et al. [21] investigated the complicated dynamics of MHD flow with mixed convection over a stretching surface. Finally, a theoretical analysis of the dynamics of ternary hybrid nanofluids was carried out by Ramzan et al. [22] while the nanofluids traversed a variety of non-isothermal and non-isosolutal geometries. This study contributed to the advancement of nanofluid research and pushed the frontiers of what is currently known in the area.

Field on unsteady hybrid nanofluid flow over an inclined rotating disk, incorporating factors like Joule heating, viscous dissipation, thermal radiation, and slip conditions, solved using the Runge-Kutta method and validated through neural networks [23]. The study by Hayat et al. [24] investigates the flow of radiative hybrid nanomaterials across a permeable curved surface, focusing on inertial and Joule heating effects. This research highlights the significance of hybrid nanofluids in enhancing thermal efficiency and mass transfer, which is crucial for various engineering applications. The findings indicate that the inclusion of nanoparticles significantly improves the thermal and flow characteristics of the fluid. The investigation of composed charged particles with ternary hybrid nanoparticles in a 3D power law model, as presented by Nazir et al. [25], highlights the significance of hybrid nanoparticles in enhancing the properties of nanofluids and their applications in various fields. This study utilizes a Galerkin algorithm to compute the behavior of these nanoparticles, emphasizing their potential in improving thermal and flow characteristics in industrial applications.

The study by Waseem et al. [26] investigates the entropy generation in magnetohydrodynamic (MHD) hybrid nanoparticles, emphasizing the effects of viscous dissipation and thermal radiation. This research contributes to understanding how these factors influence thermal performance in nanofluids, which is critical for optimizing heat transfer systems. The following sections elaborate on key aspects of this analysis. The study by Alao et al. [27] investigates the effects of thermal radiation, Soret, and Dufour on unsteady heat and mass transfer in a chemically reacting fluid past a semi-infinite vertical plate. This research highlights the complex interactions between these factors and their implications for fluid dynamics and engineering applications. The following sections elaborate on the key findings and methodologies relevant to this topic. The study of Darcy ternary hybrid nanofluid flow involving titanium dioxide (TiO_2), cobalt ferrite ($CoFe_2O_4$), and magnesium oxide (MgO) nanoparticles reveals significant enhancements in thermal and flow characteristics across various surfaces. The mathematical modeling of this flow, which incorporates factors such as heat sources, magnetic fields, and activation energy, demonstrates its applicability in engineering and medical fields. The findings indicate that the energy and mass transfer rates are influenced by the geometry of the surface and the properties of the nanofluid by Bilal et al. [28].

In a groundbreaking approach, Choi and Eastman [29] proposed the creation of a new category of heat transfer fluids through the suspension of metallic nanoparticles within formerly used fluids. Their theoretical investigation sheds light on the remarkable thermal conductivity of nanofluids that contain nanoparticles of copper, revealing the potential for significant advantages, including substantial reductions in pumping power for heat exchangers. This innovation not only enhances efficiency but also opens new avenues for engineering more effective heat transfer solutions.

As a result of the reviewed literature above, tiny or no work has explored the significance of Joule heating and Fourier heat flux on the dynamics of ternary hybrid nanofluid rotating in a circular porous disk. Having this in mind, the significance of pertinent flow parameters such as thermal radiation, magnetic field, viscous dissipation, permeability parameters are examined on velocity and temperature profiles respectively.

This type of analysis is uncharted territory in the existing literature. We delve into the dynamics of a non-Newtonian hybrid nanofluid within a permeable circular disk, revealing insights that hold significant promise for both engineering and scientific applications. For instance, the implications of thermal radiation are particularly relevant in thermal engineering, while the Lorentz force plays a crucial role in MHD accelerators and chemical catalytic reactors. This research not only broadens the horizon of nanofluid studies but also paves the way for practical innovations across various fields.

2. MATHEMATICAL MODEL

Let's consider the flow and heat transfer of MHD hybrid nanofluids in a specific setup. We consider an incompressible,

viscous, laminar, and unsteady three-dimensional flow. This flow occurs between two coaxial disks that move orthogonally to each other. An external magnetic field is applied in the z-direction. The disks have a diameter of 2r and move up and down with a standardized velocity denoted as s'(t). Additionally, the size of the disks varies with a factor of 2s(t). This analysis by neglecting the induced magnetic field, grounded in the assumption of a low Reynolds number. The physical model is framed within a cylindrical coordinate system (r,θ,z), allowing us to effectively capture the dynamics of the system. In this analysis, both viscous dissipation and Joule heating effects are excluded. Additionally, chemical reactions are not considered in the enhancement of heat transfer for the hybrid nanofluids. The velocity field of the fluid is described by $v = (u(r,z,t), v(r,z,t), w(r,z,t))$.

Figure 1 illustrates the study of nanofluids, focusing on a mathematical model for laminar, incompressible, two-dimensional flow of a ternary hybrid nanofluid, which consists of nanomaterials suspended in pure water as the base fluid. The setup features a circular porous disk, emphasizing the physical significance of the geometry in influencing fluid dynamics. The ambient temperature is denoted as T_∞, while T_W represents the wall temperature of the disk.

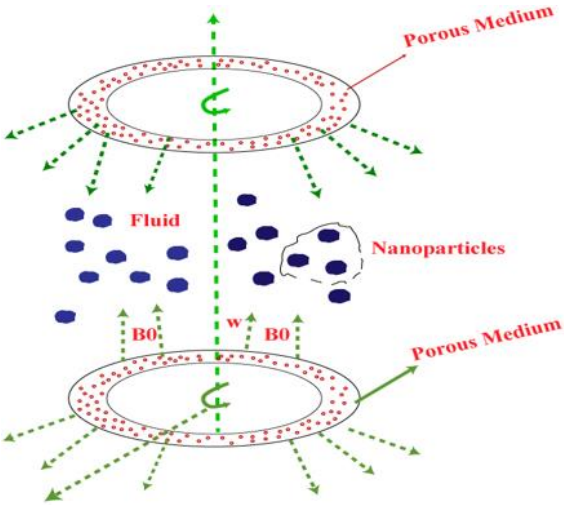

Figure 1. Visualization of the physical model

Key assumptions in this model include the effects of radiation, heat generation, Joule heating, the presence of a magnetic field, viscous dissipation, and Fourier heat flux, all of which are considered to impact the flow behavior. Both disks are rotating with an angular velocity of Ω, and the boundary layer approximation is deemed applicable in this scenario. The porous medium, depicted in the top and bottom sections of the figure, signifies a material that permits the fluid to permeate through its interconnected voids, thus enhancing the overall fluid flow and heat transfer characteristics in the system. This configuration allows for a comprehensive analysis of the interactions between the nanofluid and the disk under various thermal and flow conditions.

3. GOVERNING EQUATIONS

The governing equations [15]:

$$\frac{\partial u}{\partial r} + \frac{u}{r} + \frac{\partial w}{\partial z} = 0 \tag{1}$$

$$\begin{aligned} &\rho_{thnf}\left(u\frac{\partial u}{\partial r} - \frac{v^2}{r} + w\frac{\partial u}{\partial z}\right) + \frac{\partial p}{\partial r} \\ &= \mu_{hnf}\left(\frac{\partial^2 u}{\partial r^2} + \frac{1}{r}\frac{\partial u}{\partial r} - \frac{u}{r^2} + \frac{\partial^2 u}{\partial z^2}\right) \\ &-\sigma_{hnf}B_0^2 u - \frac{\mu_{thnf}}{K_0}u \end{aligned} \tag{2}$$

$$\begin{aligned} &\rho_{thnf}\left(u\frac{\partial v}{\partial r} - \frac{uv}{r} + w\frac{\partial v}{\partial z}\right) \\ &= \mu_{thnf}\left(\frac{\partial^2 v}{\partial r^2} + \frac{1}{r}\frac{\partial v}{\partial r} - \frac{v}{r^2} + \frac{\partial^2 v}{\partial z^2}\right) \\ &-\sigma_{thnf}B_0^2 u - \frac{\mu_{thnf}}{K_0}v \end{aligned} \tag{3}$$

$$\begin{aligned} &\rho_{thnf}\left(u\frac{\partial w}{\partial r} + w\frac{\partial w}{\partial z}\right) + \frac{\partial p}{\partial r} \\ &= \mu_{thnf}\left(\frac{\partial^2 w}{\partial r^2} + \frac{1}{r}\frac{\partial w}{\partial r} + \frac{\partial^2 w}{\partial z^2}\right) \end{aligned} \tag{4}$$

$$\begin{aligned} &(\rho.c_p)_{thnf}\left(u.\frac{\partial T}{\partial r} + w.\frac{\partial T}{\partial z}\right) + \frac{\partial p}{\partial r} \\ &= K_{thnf}\left(\frac{\partial^2 T}{\partial r^2} + \frac{1}{r}.\frac{\partial T}{\partial r} + \frac{\partial^2 T}{\partial z^2}\right) - \frac{\partial q_r}{\partial z} \\ &+Q_0.(T - T_\infty) + \frac{\mu_{thnf}}{(\rho c_p)_{thnf}}.\left(\frac{\partial u}{\partial z}\right)^2 \\ &-\Gamma_1\begin{pmatrix} u^2.\frac{\partial^2 T}{\partial r^2} + w^2.\frac{\partial^2 T}{\partial r^2} + 2u.w\frac{\partial^2 T}{\partial r \partial z} \\ +\frac{\partial T}{\partial r}\left(u\frac{\partial u}{\partial r} + w\frac{\partial w}{\partial r}\right) + \left(u.\frac{\partial u}{\partial r} + w.\frac{\partial w}{\partial r}\right)\frac{\partial T}{\partial z} \end{pmatrix} \\ &+\sigma_{thnf}B_0^2.v \end{aligned} \tag{5}$$

Subject to:

The corresponding boundary conditions for the three-dimensional flow are outlined as follows:

$$\begin{aligned} &\text{at } z = 0, u = 0, v = \Omega r, w = w_0, T = T_w \\ &\text{at } z \to \infty, u \to 0, v \to 0, T \to T_\infty, P \to P_\infty \end{aligned} \tag{6}$$

According to the study of Alao et al. [27], the radiative heat flux was described using Rosseland diffusion approximation as:

$$q_r = -\frac{4\sigma^*}{3K^*}\frac{\partial T^4}{\partial z}$$

and σ* indicate Stefan-Boltzmann constant, K* indicate mean absorption coefficient. Considering that difference in temperature occurs in the flow to be very small such that T^4 is expressed in a nonlinear form as:

$$\frac{\partial q_r}{\partial z} = \frac{\partial}{\partial z}.\left(\frac{4\sigma^*}{3K^*}.4T^3.\frac{\partial T}{\partial z}\right) \tag{7}$$

The governing flow equations PDEs are simplified using the following similarities transformations defined as:

$$\begin{aligned} &u = r.\Omega.f', v = r.\Omega g \\ &w = \sqrt{2.\Omega.\nu_f}.f, P = P_\infty + 2.\Omega.\mu_f.P(\eta) \\ &\eta = \sqrt{\frac{2.\Omega}{\nu_f}}z, \theta = \frac{(T - T_\infty)}{(T_w - T_\infty)} \end{aligned} \tag{8}$$

Table 1. Thermophysical characteristics of the base fluid and nanoparticles [15]

Properties	Thermal Conductivity	Heat Capacity	Density	Prandtl Number
Silver (Ag)	42.9*10	23.5*10	10.5*100	-
Copper (Cu)	40.1*10	38.5*10	893.3*10	-
Manganese zin ferrite $MuZnFe_2O_4$	$39*10^{-1}$	105*10	47*100	-
Kerosene oil	$15*10^{-2}$	209*10	78.3*10	21

Table 2. Nanoparticles' thermophysical characteristics

	Nanoparticles and Base Fluid Naming Convections	K(W/mk)	$c_p(I/kgk)$	$\rho(\frac{kg}{m^3})$	Shapes of Naoparticles
Hybrid nanofluid 1	Aluminum oxide Al_2O_3 (0.05%)	4*10	$7.65*10^2$	397*10	Platelet
	Carbon nanotubes (0.01%)	$30074*10^{-1}$	410	$21*10^2$	Spherical
	Graphene (0.05%)	$5*10^2$	790	$22*10^2$	Cylindrical
Hybrid naofluid 2	Silver (Ag) (0.05%)	42.9*10	235	$105*10^2$	Platelet
	Copper oxide CuO (0.01%)	2*10	535.6	$65*10^2$	Spherical
	Copper Cu (0.05%)	$4*10^2$	385	893.3*10	Cylindrical
Base fluid	Water H_2O	$623*10^{-3}$	4.179	997.1	

By applying the above transformations, the transformed equations becomes:

$$\frac{M_1}{M_4}(2.f\cdot f''-(f')^2+g^2)+2\cdot f'''-\frac{M_5}{M_4}\cdot M\cdot f'-\frac{1}{P_0}\cdot f'=0 \quad (9)$$

$$\frac{M_1}{M_4}(2\cdot f\cdot g'-2\cdot f'\cdot g)+2\cdot g''-\frac{M_5}{M_4}\cdot M\cdot f'-\frac{1}{P_0}\cdot f'=0 \quad (10)$$

$$\frac{M_2}{M_3}f.\theta'+\frac{1}{Pr}\left(\theta''+\frac{4.Nr}{3.M_3}\frac{d}{d\eta}\left(1+\theta(\eta)(\theta_w-1)\right)^3\frac{d\theta(\eta)}{d\eta}\right)+\frac{M_2}{M_3}f\theta'+PrQr(f^2\theta''+ff'\theta')+\Delta_r\theta+Ec(f'')^2+EcM(f')^2=0 \quad (11)$$

Subject to:

$$f=-S, f'=0, g=1, \theta=1, at\ \eta=0 \quad (12)$$

$$f'\to 0, g\to 0, \theta\to 0, at\ \eta\to\infty \quad (13)$$

where, defined parameters are:

$$M_1=\frac{\rho_{hnf}}{\rho_f}, M_2=\frac{(\rho c_p)_{hnf}}{(\rho c_p)_f}, M_3=\frac{K_{hnf}}{K_f}$$
$$M_4=\frac{\mu_{hnf}}{\mu_f}, M_5=\frac{\sigma_{hnf}}{\sigma_f}$$

Table 1 represents the aforementioned table delineates the thermophysical properties of the base fluid and various nanoparticles, presenting critical parameters such as thermal conductivity, heat capacity, density, and the Prandtl number for each material listed.

Table 2 delineates the thermophysical characteristics of diverse nanoparticles in conjunction with water functioning as the base fluid. Hybrid Nanofluid 1 encompasses aluminum oxide (Al_2O_3) exhibiting a thermal conductivity of 4 W/m·K (in a platelet morphology), carbon nanotubes demonstrating a conductivity of 3007.4 W/m·K (in a spherical morphology), and graphene presenting a thermal conductivity of 500 W/m·K (in a cylindrical morphology). Hybrid Nanofluid 2 comprises silver (Ag) with a thermal conductivity of 42.9 W/m·K (in a platelet morphology), copper oxide (CuO) with a conductivity of 2 W/m·K (in a spherical morphology), and copper (Cu) exhibiting a thermal conductivity of 400 W/m·K (in a cylindrical morphology). For purposes of comparison, water (H_2O) is utilized as the base fluid, possessing a thermal conductivity of 0.623 W/m·K. This dataset underscores the potential for enhanced thermal performance of hybrid nanofluids relative to the base fluid.

For C_g, C_f and Nu the relevant engineering quantities are defined, correspondingly.

$$C_g=\left(\frac{(1-\phi_1-\phi_2-\phi_3)^{-2.5}}{(1-\phi_1-\phi_2-\phi_3)+\phi_1\left(\frac{\rho_1}{\rho_f}\right)}+\phi_2\left(\frac{\rho_2}{\rho_f}\right)+\phi_3\left(\frac{\rho_3}{\rho_f}\right)\right)g'(0)$$

$$c_f=\left(\frac{(1-\phi_1-\phi_2-\phi_3)^{-2.5}}{(1-\phi_1-\phi_2-\phi_3)+\phi_1\left(\frac{\rho_1}{\rho_f}\right)}+\phi_2\left(\frac{\rho_2}{\rho_f}\right)+\phi_3\left(\frac{\rho_3}{\rho_f}\right)\right)f''(0)$$

$$Nu=\frac{Nu}{\sqrt{Re_z}}=\frac{K_{hnf}}{K_f}\left(1+\frac{4Nr}{4M_3}\left(1+(\theta_w-1)\theta(0)\right)^3\right)\theta'(0)$$

4. METHODOLOGY

A detailed numerical scheme was developed on the transformed Eqs. (1)-(5) subject to (6). Boundary value problem using Runge-Kutta alongside shooting technique was employed to solve the transformed ODEs. In MATLAB was employed on the systems of equations. It was observed to be very easy and converges easily at a convergence rate of 10^{-6}. An iteration structure was employed on the nonlinear systems of equation. The shooting techniques was employed by first changing the transformed third order equation into a first order equations as follows.

Table 3. All parameters with their values

M	P_o	Pr	N_r	Δ_r	E_c	Q_r	$-f'(0)$	Nu
0.2							1.919901383	0.537359717
0.4							1.569705275	0.537359717
0.6							1.281962577	0.537359717
	0.5						2.90910142	0.711182647
	1						3.156210184	0.711182647
	2						4.392518985	0.711182647
		0.71					1.69445097	0.719327227
		3					1.57156978	1.030344358
		7					1.513094986	1.341806231
			0				2.082554162	0.494919237
			0.5				2.199516306	0.501766431
			1				2.272640918	0.516831295
				0.3			2.026677179	0.130418918
				0.6			2.24022877	0.203102504
				0.9			2.453780362	0.536623926
					0.1		2.25059991	0.014150472
					0.3		2.582127256	0.500244761
					0.5		2.913654601	1.014639994
						1	2.593332016	0.408670108
						2	3.385603349	1.509764021
						3	4.177874682	2.610857933

$$f = y_1,\ \frac{df}{d\eta} = \frac{dy_1}{d\eta} = y_2,\ \frac{d^2 f}{d\eta^2} = \frac{d}{\eta}\left(\frac{dy_1}{d\eta}\right) = \frac{dy_2}{d\eta} = y_3,$$

$$\frac{d^3 f}{d\eta^3} = \frac{d}{\eta}\left(\frac{dy_2}{d\eta}\right) = \frac{dy_3}{d\eta}$$

$$g = y_4,\quad \frac{dg}{d\eta} = \frac{dy_4}{d\eta} = y_5,\quad \frac{d^2 g}{d\eta^2} = \frac{d}{\eta}\left(\frac{dy_4}{d\eta}\right) = \frac{dy_5}{d\eta}$$

$$\theta = y_6,\quad \frac{d\theta}{d\eta} = \frac{dy_6}{d\eta} = y_7,\quad \frac{d^2\theta}{d\eta^2} = \frac{d}{\eta}\left(\frac{dy_6}{d\eta}\right) = \frac{dy_7}{d\eta}$$

$$\frac{M_1}{M_2}\left(2y_1y_3 - (y_2)^2 + (y_4)^2\right) + 2\frac{dy_3}{d\eta} - \frac{M_5}{M_4}My_2 = 0$$

$$\frac{M_1}{M_2}\left(2y_1y_5 - 2y_2y_4\right) + 2\frac{dy_5}{d\eta} - \frac{M_5}{M_4}My_4 = 0$$

$$\frac{M_2}{M_3}y_1y_7 + \frac{1}{Pr}\left(\frac{dy_7}{d\eta} + \frac{4Nr}{3M_3}\frac{d}{d\eta}\left(1 + y_6(\theta_w - 1)\right)^3 y_7\right) + \frac{M_2}{M_3}y_1y_7$$

$$+ \mathrm{PrQr}\left((y_1)^2\frac{dy_7}{d\eta} + y_1y_7y_2\right) + \Delta_r y_6 + Ec(y_3)^2 = 0$$

$$\frac{dy_3}{d\eta} = \frac{\frac{M_5}{M_4}My_2 - \frac{M_1}{M_2}\left(2y_1y_3 - (y_2)^2 + (y_4)^2\right)}{2}$$

$$\frac{dy_5}{d\eta} = \frac{\frac{M_5}{M_4}My_4 - \frac{M_1}{M_2}\left(2y_1y_5 - 2y_2y_4\right)}{2}$$

$$\frac{dy_7}{d\eta} = \frac{-\frac{M_2}{M_3}y_1y_7 - \frac{4Nr}{3M_3}\frac{d}{d\eta}\left(1 + y_6(\theta_w - 1)\right)^3 y_7}{\frac{1}{\mathrm{Pr}} + \mathrm{PrQr}(y_1)^2}$$

$$- \frac{\frac{M_2}{M_3}y_1y_7 - \mathrm{PrQr}\,y_1y_7y_2 - \Delta_r y_6 - Ec(y_3)^2}{\frac{1}{\mathrm{Pr}} + \mathrm{PrQr}(y_1)^2}$$

The Table 3 delineates a spectrum of parameters pertinent to fluid dynamics and thermal transfer, encompassing viscosity (M) values ranging from 0.2 to 3, supplemented by associated entries for additional unspecified parameters (P_o, Pr, N_r, Δ_r, E_c). It incorporates dimensionless metrics such as Q_r, which ostensibly signifies a heat transfer rate, and $-f'(0)$, presumably a derivative evaluated at a particular point, in conjunction with the Nusselt number (Nu) that serves to differentiate between convective and conductive heat transfer mechanisms. The data elucidates patterns in Q_r and Nu in response to variations in M and other parameters, thereby underscoring potential correlations within the realm of fluid dynamics.

5. RESULTS WITH DISCUSSION

In the numerical simulation of the flow Eqs. (1)-(5) alongside the boundary constraints Eq. (6) and Eq. (7), the control parameters implemented are:

$\mathrm{Pr}=71*10^{-2}$, $E_c=6*10^{-1}$, $\mathrm{Sc}=61*10^{-2}$, $\mathrm{Cr}=9*10^{-1}$, $N_r=0.9$, M=1.0

The numerical values are kept constant for tables and graphical results unless otherwise stated. The complex dynamics of fluid flow phenomena can be better understood by observing how controlled parameters affect the velocity and temperature profiles. By comparing the results to those of other studies, this research proves that its methodology is sound.

When it comes to tables and graphical results, the numerical values are maintained at a constant level unless otherwise specified. A better understanding of the complex dynamics of fluid flow phenomena can be gained via the examination of the influence of controllable parameters on the velocity and temperature profiles. A comparison is made between the findings of this research with those of earlier works in the field of literature in order to demonstrate that the way of approach is appropriate.

Figure 2 demonstrates how the thermal radiation parameter (R) affects the velocity and temperature profiles within the fluid system. As R increases, a marked improvement in both

profiles is evident, underscoring the significant role of thermal radiation in fluid dynamics. This effect is particularly pronounced in scenarios where the fluid temperature is higher, making thermal radiation increasingly significant.

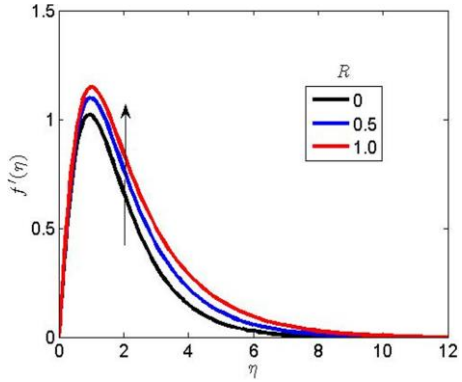

(a) The velocity profiles

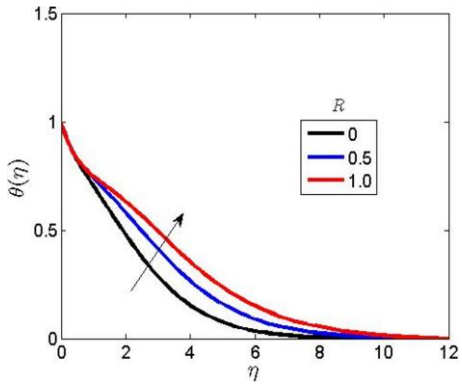

(b) The velocity and temperature landscapes

Figure 2. Effect of thermal radiation parameter on the velocity and temperature profiles

Thermal radiation, represented by parameter R, quantifies the heat energy transferred via radiation from the fluid to its surroundings or vice versa. As R increases, the fluid system experiences more effective thermal radiation effects, which results in several key outcomes:

Increased temperature profiles: Higher values of R correspond to enhanced radiative heat transfer, which contributes to a complete improve in the temperature of the fluid. The additional thermal radiation effectively elevates the thermal energy within the system, leading to higher temperature profiles throughout the fluid.

Enhanced velocity profiles: The increase in temperature due to higher thermal radiation influences the fluid's dynamic behaviour. As the fluid temperature rises, it affects the fluid's viscosity and density, potentially leading to increased convective currents and enhanced velocity profiles

Thicker thermal boundary layer: An increase in the amount of thermal radiation that is present causes the thermal state of the fluid environment to become more intense. The thickness of the thermal boundary layer is increased as a result of this heightened thermal state having a contributing factor. To put it simply, the thermal boundary layer thickens as more thermal energy is radiated and absorbed. This is a reflection of the increased heat transfer and temperature gradients that occur inside the fluid.

Figure 3 depicts the effect of the Fourier heat flux relaxation parameter (Q_r) on both the velocity and temperature profiles within the fluid system. As illustrated, an increase in the value of Q_r results in a notable enhancement of both temperature and velocity profiles.

The Fourier heat flux relaxation parameter (Q_r) quantifies the extent to which the heat flux in the fluid system deviates from the classical Fourier heat conduction model, considering relaxation effects. This parameter is crucial in analysing thermal dynamics, especially in systems where the heat flux does not instantaneously adjust to changes in temperature gradients. Key observations and physical implications from Figure 3 include:

Increased temperature profiles: As Q_r increases, the relaxation effects in heat flux become increasingly pronounced. This enhanced relaxation allows the fluid to more effectively absorb and distribute thermal energy, leading to elevated temperature profiles. In essence, higher values of Q_r boost the fluid's capacity to retain and manage heat, ultimately raising the overall temperature throughout the system.

Enhanced velocity profiles: The increase in temperature due to higher Q_r also affects the velocity profiles. Elevated temperatures often lead to reduced fluid viscosity, which enhances convective currents and promotes higher velocity profiles. Therefore, as Q_r increases and temperature rises, the fluid's velocity profile is also enhanced.

Thicker boundary layers: The outcomes shown in Figure 3 indicate that higher values of Q_r contribute to an expansion of both the momentum and thermal bound layers. Additionally, the improved heat flow relaxation makes it possible for a more gradual thermal adjustment to take place within the fluid, which results in the thermal boundary layer being thicker. Similarly, the momentum boundary layer thickens as increased temperature affects fluid dynamics, leading to greater momentum diffusion near the boundary.

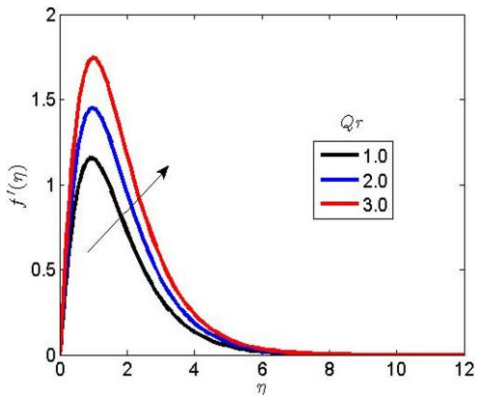

(a) The velocity profiles

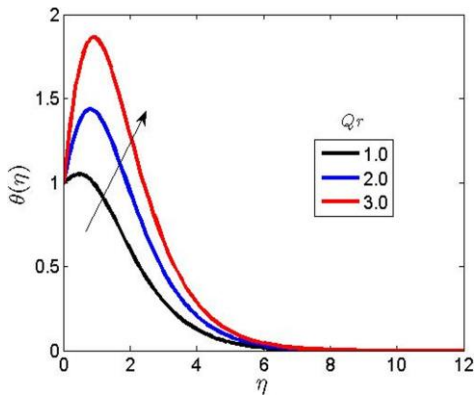

(b) The temperature profile

Figure 3. Varying the Fourier heat flux relaxation parameter alters the temperature and velocity profiles

Figure 4 illustrates how the Prandtl number (Pr) influences the temperature and velocity reports in a fluid system. The definition of this dimensionless number is the ratio of momentum diffusivity, also known as kinematic viscosity, to thermal diffusivity. This ratio is mathematically stated as Pr = α/v. where α represents thermal diffusivity. The Prandtl number is vital for understanding the interaction between fluid dynamics and heat transfer, offering valuable insights into the relative significance of momentum transfer in comparison to heat transfer within the fluid. Key findings and physical interpretations from Figure 4 are as follows:

Decreased temperature profiles: An increase in the Prandtl number (Pr) is observed to lower the temperature profiles in the fluid. This occurs because a higher Prandtl number indicates higher viscosity relative to thermal diffusivity. As a result, the fluid's ability to conduct heat is reduced compared to its ability to diffuse momentum. The reduced thermal conductivity results in less efficient heat transfer, which causes a decrease in the temperature profiles within the boundary layer.

Decreased velocity profiles: Similarly, a higher Prandtl number mains to a drop in the velocity shapes. The increased viscosity (due to a higher Prandtl number) impedes fluid motion, resulting in a drop in the velocity. The fluid's resistance to shear stresses increases, which affects its convective motion and thus lowers the velocity profiles.

Boundary layer thickness: When Pr is greater than 1, it implies that the fluid has high viscosity and relatively low thermal diffusivity. This scenario results in a weaker thermal frontier layer because the reduced heat transfer efficiency causes less thermal penetration into the fluid. Conversely, the momentum frontier layer also becomes thinner as higher viscosity reduces the extent of momentum diffusion near the boundary.

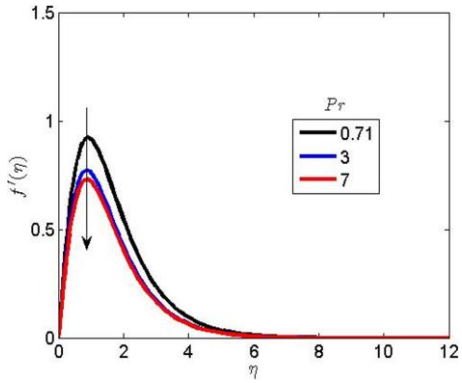

(a) The velocity profile

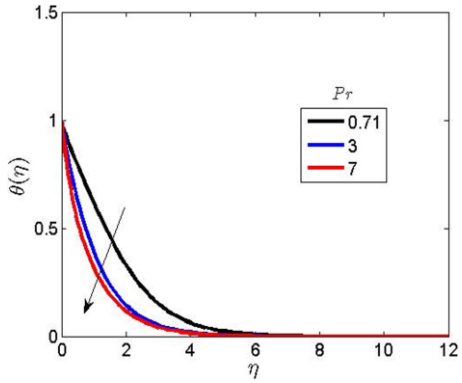

(b) The thermal landscape

Figure 4. Influence of the Prandtl number on the flow's velocity and thermal profiles

Figure 5 illustrates the profound impact of the magnetic parameter (M) on the velocity profile of a fluid. The presence of an imposed magnetic field significantly alters the thermophysical properties of the fluid, particularly when the Prandtl number (Pr) exceeds 1, indicating a highly conductive medium. In such scenarios, the electromagnetic forces exerted by the magnetic field become crucial in governing the fluid's motion. The application of the magnetic field results in the production of a drag force, which acts in opposition to the movement of the fluid that provides electrical conductivity. As a result of this drag force, the velocity of the fluid is effectively slowed down, which ultimately results in a thinner momentum boundary layer. owing to the fact that there is no slip condition, the velocity of the fluid changes from zero at the boundary to the velocity of the free stream in the region that is referred to as the momentum boundary layer. As the magnetic parameter increases, the drag force intensifies, further constraining the fluid's flow and altering its velocity profile.This interaction between the magnetic field and the fluid dynamics highlights the intricate relationship between electromagnetic forces and fluid behavior. The result is a complex interplay In this context, the magnetic field not only has an effect on the velocity, but it also plays a significant part in the total thermal and dynamic properties of the fluid system. When it comes to applications in domains such as MHD, having a solid understanding of these effects is absolutely necessary., where the behavior of conductive fluids in magnetic fields is of paramount importance.

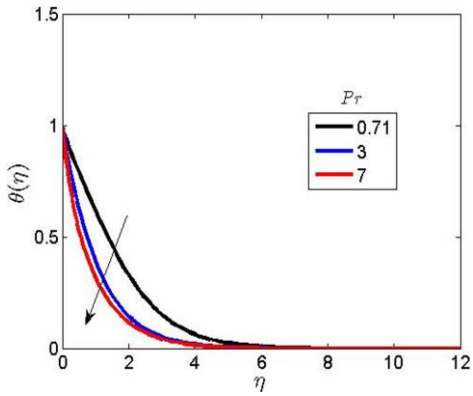

Figure 5. Impact of the magnetic parameter on velocity dynamics

Figure 6 reveals the impact that the Eckert number, a crucial metric that measures viscous dissipation, has on the velocity and temperature profiles that are present within the fluid system. By capturing the equilibrium between the kinetic energy of the fluid and the thermal energy that is generated by viscous friction, this fascinating number captures the essence of the situation. Because of the internal friction of the electrically conductive fluid, the Eckert number increases, which indicates that a greater amount of mechanical energy is being converted into heat. The upshot of this change is a discernible rise in temperature over the entirety of the fluid, which in turn generates a cascade effect that simultaneously improves the velocity profiles of the fluid. When it comes down to it, the interaction of increased viscous dissipation not only raises the temperature of the fluid but also quickens its flow. This highlights the significant role that frictional heating plays in changing the thermal and dynamic behavior of the fluid system.

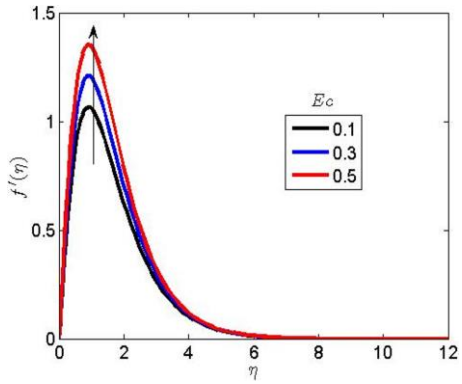

(a) The velocity profiles

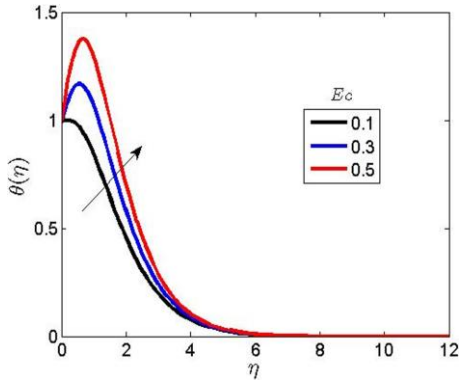

(b) The temperature landscape

Figure 6. Influence of the eckert number on velocity and temperature distributions

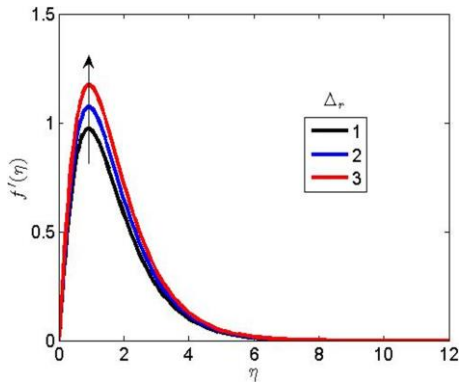

(a) The velocity profiles

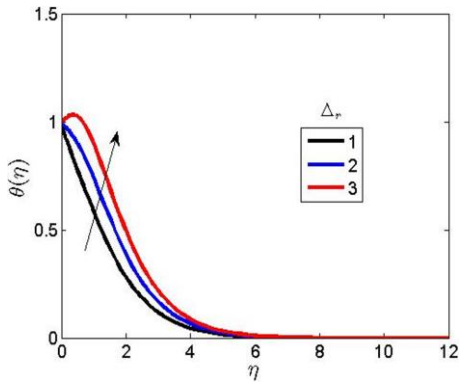

(b) The temperature profile

Figure 7. Effect of heat generation parameter on the velocity and temperature profiles

Figure 7 delves into the impact of the heat generation parameter on the velocity and temperature profiles within the boundary layer, presenting detailed findings from this investigation. To illustrate the effects of heat generation, the parameter is plotted against both velocity and temperature profiles. As illustrated in Figure 7, increases in the heat generation parameter lead to elevations in the velocity and temperature profiles within the boundary layer. This phenomenon occurs because the conversion of kinetic energy into thermal energy is closely linked to heat generation.

Specifically, the dissipation of kinetic energy due to viscous forces increases heat production within the boundary layer. This increase in heat generation enhances the thermal energy within the fluid, which in turn raises the temperature profile. The higher temperature of the fluid can lead to stronger convective currents and reduced viscosity, further elevating the velocity profile. Simultaneously, the additional thermal energy contributes to an increase in the velocity profile.

Thus, Figure 7 underscores the significant role of heat generation in influencing both the thermal and dynamic characteristics of the boundary layer, reflecting the interdependence between the loss of kinetic energy and the increase in thermal energy.

6. CONCLUSION

The analysis of heat flux and joule heating on the dynamics of heat transmission on ternary hybrid nanofluid rotating in a circular porous disk has been considered. The circular disk at the upper and lower region was examined to be porous. The radiative heat flux was simplified by employing the Rosseland diffusion model in examining its behavior on the fluid dynamics. Around the layers, all fluid properties such as viscosity and thermal conduction are examined to be considered. The Runge-Kutta alongside shooting technique was employed to solve the transformed ODEs. The ket findings in this study are as stated below:

(i) According to the findings of the study, thermal radiation can greatly increase the amount of heat transfer that occurs within the boundary layer. This, in turn, can result in a large increase in both the temperature profile and the overall thickness of the thermal boundary layer.

(ii) A Lorentz force is produced as a result of the application of a magnetic field, which effectively restricts the velocity profile and makes the motion of the fluid more restricted.

(iii) As permeability increases, the flow of fluid particles becomes more pronounced. Consequently, a greater permeability parameter results in enhanced fluid velocity within the boundary layer.

(iv) A higher viscous dissipation parameter (Eckert number) generates heat energy, resulting in increased fluid temperature and velocity.

(v) The velocity and temperature profiles are shown to grow exponentially with a large increase of the heat generation parameter.

(vi) It was found that the Sherwood number and the concentration boundary layer thickness are both reduced with an increase in the chemical reaction parameter.

Real world applications: Point (i) supports to Boosts heat absorption efficiency in solar Thermal Collectors. Pont (ii) supports to control the flow of molten metals and improve mixing in foundries, enhancing the quality of castings. Point (iii) supports to Increasing the permeability of reservoir rocks can improve the flow of oil, leading to more efficient

extraction. Point (iv) used in In high-speed turbomachinery, such as turbines and compressors, managing viscous dissipation can help control temperature and improve performance. Understanding how viscous dissipation affects fluid dynamics helps in optimizing the design for better efficiency and reduced energy losses. Point (v) used in In exothermic chemical reactions, increasing heat generation can enhance reaction rates and improve reactor performance. Higher temperatures and velocities can lead to more efficient mixing and faster processing.point(iv) related to In catalytic processes, a higher chemical reaction parameter can improve the efficiency of mass transfer by reducing the concentration boundary layer. This leads to better utilization of the catalyst and improved reaction rates.

REFERENCES

[1] Raza, Q., Wang, X., Ali, B., Eldin, S.M., Yang, H., Siddique, I. (2023). Role of nanolayer on the dynamics of tri-hybrid nanofluid subject to gyrotactic microorganisms and nanoparticles morphology vis two porous disks. Case Studies in Thermal Engineering, 51: 103534. https://doi.org/10.1016/j.csite.2023.103534

[2] Idowu, A.S., Falodun, B.O. (2020). Variable thermal conductivity and viscosity effects on non-Newtonian fluids flow through a vertical porous plate under Soret-Dufour influence. Mathematics and Computers in Simulation, 177: 358-384. https://doi.org/10.1016/j.matcom.2020.05.001

[3] Salah, Y., Al Mukbel, O., Sabsabi, Y., Saranya, S., Al-Mdallal, Q.M., Mukhamedova, F. (2023). Influence of PST and PHF heating conditions on the swirl flow of Al+ Mg+ TiO2 ternary hybrid water-ethylene glycol based nanofluid with a rotating cone. International Journal of Thermofluids, 19: 100371. https://doi.org/10.1016/j.ijft.2023.100371

[4] Sajjan, K., Shah, N.A., Ahammad, N.A., Raju, C.S.K., Kumar, M.D., Weera, W. (2022). Nonlinear Boussinesq and Rosseland approximations on 3D flow in an interruption of Ternary nanoparticles with various shapes of densities and conductivity properties. AIMS Math, 7(10): 18416-18449. https://doi.org/10.3934/math.20221014

[5] Khan, M.R., Ahammad, N.A., Alhazmi, S.E., Ali, A., Abdelmohimen, M.A.H., Allogmany, R., Tag-Eldin, E., Yassen, M.F. (2022). Energy and mass transport through hybrid nanofluid flow passing over an extended cylinder with the magnetic dipole using a computational approach. Frontiers in Energy Research, 10: 980042. https://doi.org/10.3389/fenrg.2022.980042

[6] Haq, I., Bilal, M., Ahammad, N.A., Ghoneim, M.E., Ali, A., Weera, W. (2022). Mixed convection nanofluid flow with heat source and chemical reaction over an inclined irregular surface. ACS Omega, 7(34): 30477-30485. https://doi.org/10.1021/acsomega.2c03919

[7] Gladys, T., Reddy, G.R. (2022). Contributions of variable viscosity and thermal conductivity on the dynamics of non-Newtonian nanofluids flow past an accelerating vertical plate. Partial Differential Equations in Applied Mathematics, 5: 100264. https://doi.org/10.1016/j.padiff.2022.100264

[8] Gurrampati, V.R.R., Vijaya, K. (2022). The Buongiorno model with Brownian and thermophoretic diffusion for MHD casson nanofluid over an inclined porous surface. Journal of Naval Architecture and Marine Engineering, 19(1): 31-45. https://doi.org/10.3329/jname.v19i1.50863

[9] Alkuhayli, N.A.M. (2023). Enhancing the heat transfer due to hybrid nanofluid flow induced by a porous rotary disk with hall and heat generation effects. Mathematics, 11(4): 909. https://doi.org/10.3390/math11040909

[10] Mishra, N.K., Sharma, P., Sharma, B.K., Almohsen, B., Pérez, L.M. (2024). Electroosmotic MHD ternary hybrid Jeffery nanofluid flow through a ciliated vertical channel with gyrotactic microorganisms: Entropy generation optimization. Heliyon, 10(3): e25102. https://doi.org/10.1016/j.heliyon.2024.e25102

[11] Alhowaity, A., Bilal, M., Hamam, H., Alqarni, M.M., Mukdasai, K., Ali, A. (2022). Non-Fourier energy transmission in power-law hybrid nanofluid flow over a moving sheet. Scientific Reports, 12(1): 10406. https://doi.org/10.1038/s41598-022-14720-x

[12] Alharbi, K.A.M., Bilal, M., Ali, A., Eldin, S.M., Soliman, A.F., Rahman, M.U. (2023). Stagnation point flow of hybrid nanofluid flow passing over a rotating sphere subjected to thermophoretic diffusion and thermal radiation. Scientific Reports, 13(1): 19093. https://doi.org/10.1038/s41598-023-46353-z

[13] Kanwal, S., Shah, S.A.A., Bariq, A., Ali, B., Ragab, A.E., Az-Zo'bi, E.A. (2023). Insight into the dynamics of heat and mass transfer in nanofluid flow with linear/nonlinear mixed convection, thermal radiation, and activation energy effects over the rotating disk. Scientific Reports, 13(1): 23031. https://doi.org/10.1038/s41598-023-49988-0

[14] Tharapatla, G., RajKumari, P., Ramana Reddy, G.V. (2021). Effects of heat and mass transfer on MHD nonlinear free convection non-Newtonian fluids flow embedded in a thermally stratified porous medium. Heat Transfer, 50(4): 3480-3500. https://doi.org/10.1002/htj.22037

[15] Alqawasmi, K., Alharbi, K.A.M., Farooq, U., Noreen, S., Imran, M., Akgül, A., Kanan, M., Asad, J. (2023). Numerical approach toward ternary hybrid nanofluid flow with nonlinear heat source-sink and fourier heat flux model passing through a disk. International Journal of Thermofluids, 18: 100367. https://doi.org/10.1016/j.ijft.2023.100367

[16] Famakinwa, O.A., Koriko, O.K., Adegbie, K.S. (2022). Effects of viscous dissipation and thermal radiation on time dependent incompressible squeezing flow of CuO−Al_2O_3/water hybrid nanofluid between two parallel plates with variable viscosity. Journal of Computational Mathematics and Data Science, 5: 100062. https://doi.org/10.1016/j.jcmds.2022.100062

[17] Choudhary, S., Mehta, R., Alessa, N., Jangid, S., Venkateswar Reddy, M. (2023). Thermal analysis on kerosene oil-based two groups of ternary hybrid nanoparticles (CNT-Gr-Fe_3O_4 and MgO-Cu-Au) mix flow over a bidirectional stretching sheet: A comparative approach. Journal of Engineering, 2023(1): 8828300. https://doi.org/10.1155/2023/8828300

[18] Adnan, Nadeem, A., Mahmoud, H.A., Ali, A., Eldin, S.M. (2023). Significance of Koo-Kleinstreuer-Li model for thermal enhancement in nanofluid under magnetic field and thermal radiation factors using LSM. Advances in Mechanical Engineering, 15(10): 16878132231206906.

https://doi.org/10.1177/16878132231206906
[19] Algehyne, E.A., Lone, S.A., Raizah, Z., Eldin, S.M., Saeed, A., Galal, A.M. (2023). Mechanical characteristics of MHD of the non-Newtonian magnetohydrodynamic Maxwell fluid flow past a bi-directional convectively heated surface with mass flux conditions. Frontiers in Materials, 10: 1133133. https://doi.org/10.3389/fmats.2023.1133133
[20] Ramzan, M., Dawar, A., Saeed, A., Kumam, P., Watthayu, W., Kumam, W. (2021). Heat transfer analysis of the mixed convective flow of magnetohydrodynamic hybrid nanofluid past a stretching sheet with velocity and thermal slip conditions. Plos One, 16(12): e0260854. https://doi.org/10.1371/journal.pone.0260854
[21] Bayones, F.S., Nisar, K.S., Khan, K.A., Raza, N., Hussien, N.S., Osman, M.S., Abualnaja, K.M. (2021). Magneto-hydrodynamics (MHD) flow analysis with mixed convection moves through a stretching surface. AIP Advances, 11(4): 045001. https://doi.org/10.1063/5.0047213
[22] Ramzan, M., Kumam, P., Lone, S.A., Seangwattana, T., Saeed, A., Galal, A.M. (2023). A theoretical analysis of the ternary hybrid nanofluid flows over a non-isothermal and non-isosolutal multiple geometries. Heliyon, 9(4): e14875. https://doi.org/10.1016/j.heliyon.2023.e14875
[23] Ali, I., Gul, T., Khan, A. (2023). Unsteady hydromagnetic flow over an inclined rotating disk through neural networking approach. Mathematics, 11(8): 1893. https://doi.org/10.3390/math11081893
[24] Hayat, A.U., Ullah, I., Khan, H., Alam, M.M., Hassan, A.M., Khan, H. (2023). Numerical analysis of radiative hybrid nanomaterials flow across a permeable curved surface with inertial and Joule heating characteristics. Heliyon, 9(11): e21452. https://doi.org/10.1016/j.heliyon.2023.e21452
[25] Nazir, U., Mukdasai, K., Sohail, M., Singh, A., Alosaimi, M.T., Alanazi, M., Tulu, A. (2023). Investigation of composed charged particles with suspension of ternary hybrid nanoparticles in 3D-power law model computed by Galerkin algorithm. Scientific Reports, 13(1): 15040. https://doi.org/10.1038/s41598-023-41449-y
[26] Waseem, F., Sohail, M., Ilyas, N., Awwad, E.M., Sharaf, M., Khan, M.J., Tulu, A. (2024). Entropy analysis of MHD hybrid nanoparticles with OHAM considering viscous dissipation and thermal radiation. Scientific Reports, 14(1): 1096. https://doi.org/10.1038/s41598-023-50865-z
[27] Alao, F.I., Fagbade, A.I., Falodun, B.O. (2016). Effects of thermal radiation, Soret and Dufour on an unsteady heat and mass transfer flow of a chemically reacting fluid past a semi-infinite vertical plate with viscous dissipation. Journal of the Nigerian mathematical Society, 35(1): 142-158. https://doi.org/10.1016/j.jnnms.2016.01.002
[28] Bilal, M., Ullah, I., Alam, M.M., Weera, W., Galal, A.M. (2022). Numerical simulations through PCM for the dynamics of thermal enhancement in ternary MHD hybrid nanofluid flow over plane sheet, cone, and wedge. Symmetry, 14(11): 2419. https://doi.org/10.3390/sym14112419
[29] Choi, S.U., Eastman, J.A. (1995). Enhancing thermal conductivity of fluids with nanoparticles (No. ANL/MSD/CP-84938; CONF-951135-29). Argonne National Lab.(ANL), Argonne, IL (United States).

NOMENCLATURE

(u, v, w)	Velocity components in (r, ϕ, z) direction
P	Fluid pressure
ρ_{hnf}	Density of hybrid nanofluid
μ_{hnf}	Dynamic viscosity of hybrid nanofluid
σ_{hnf}	Electrical conductivity of hybrid nanofluid
B_0	Magnetic field strength
c_p	Specific heat at constant pressure
K_{hnf}	Thermal conductivity of hybrid nanofluid
T	Fluid temperature
q_r	Radiative heat flux
Q_0	Heat generation coefficient
T_∞	Free stream temperature
Γ_1	Fourier heat flux coefficient
Ω	Angular velocity
T_w	Wall temperature
P_∞	Free stream pressure